

J. MIETTINEN\*, G. VASSILEV\*\*

## THERMODYNAMIC DESCRIPTION OF TERNARY Fe-B-X SYSTEMS. PART 1: Fe-B-Cr

### OPIS TERMODYNAMICZNY TRÓJSKŁADNIKOWYCH UKŁADÓW Fe-B-X. CZĘŚĆ 1: Fe-B-Cr

A thermodynamic description of the Fe-B-Cr system is developed in the context of a new Fe-B-X (X = Cr, Ni, Mn, Si, Ti, V, C) database. The thermodynamic parameters of the binary sub-systems, Fe-B, Fe-Cr and B-Cr, are taken from earlier assessments slightly modifying the Fe-B and B-Cr descriptions, and those of the ternary system are optimized in this study using experimental thermodynamic and phase equilibrium data from the literature. The solution phases are described using substitutional solution model. The borides are treated as stoichiometric or semi-stoichiometric phases and described with two-sublattice models.

*Keywords:* phase diagrams; thermodynamic modelling; Fe-based systems; Fe-B-X systems thermodynamic database; Fe-B-Cr system

Przedstawiono termodynamiczny opis trójskładnikowego układu Fe-B-Cr w kontekście bazy danych dla układów Fe-B-X (X = Cr, Ni, Mn, Si, Ti, V, C). Parametry termodynamiczne dwuskładnikowych stopów Fe-Mn, Fe-B i Mn-B zostały zaczerpnięte z wcześniejszych opracowań, przy tym opisy Fe-B i B-Cr zostały nieznacznie zmodyfikowane. Parametry dla układu Fe-Mn-B zostały zoptymalizowane w tej pracy w oparciu o eksperymentalne równowagi fazowe i dane termodynamiczne zaczerpnięte z literatury. Roztwory stałe opisano przy użyciu modelu roztworu substytucyjnego, a borki traktowane są jako fazy stechiometryczne lub półstechiometryczne opisane przy użyciu modelu dwu podsieci.

### 1. Introduction

Carbon and nitrogen are known to fill the interstitial sites of the disordered solid solution structures, e.g., bcc, fcc and hcp. Although boron diffusivity in disordered phases indicates that interstitial filling could be possible [1], there is no clear experimental evidence. The purpose of this study is to initiate a project aiming to develop a thermodynamic database for boron containing iron-based systems, (Fe-B-X), where boron is treated as a substitutional component. Therefore, a series of thermodynamic descriptions of Fe-B systems alloyed with fourth period transition metal (i.e. X = Ti, V, Cr, Mn etc.) will be presented. The goal is to develop a simple and compatible thermodynamic database for steels, which provides important and practical input data for thermodynamic-kinetic models simulating their solidification. Two other elements (C and Si) are also included in the database because of their importance for the steels.

In this first paper, a thermodynamic description for the Fe-B-Cr system is performed using the experimental thermodynamic and phase equilibrium data from the literature. The system was recently assessed by Yamada et al. [2], but this description could not be used directly since its binary Fe-B and B-Cr data differs from those of the current (under way

to be published) database on Fe-B-X systems. Moreover the current Fe-B-Cr description has a slightly stronger focus on alloys with lower boron content (steels) than [2]. The differences between the results of the current study and those of Yamada et al. [2] are discussed in Section 3 (Results).

The binary thermodynamic data used in the Fe-B-Cr description presented in this work is taken from Halletmans et al. [3] for Fe-B, from Lee [4] for Fe-Cr, and from Campbel and Kattner [5] for B-Cr system. The descriptions of bcc, fcc and FeB phases from [3] and bcc, CrB and Cr<sub>4</sub>B from [5], however, were slightly modified during the database development.

In the case of the binary Fe-B system, the highest boron content of the bcc and fcc phases was slightly increased, while the stabilities of CrB and Cr<sub>4</sub>B in the B-Cr system were slightly changed to improve the agreement with the experimental data. In addition, the bcc phase of the B-Cr system was re-modeled since Campbel and Kattner [5] treated B as an interstitial component. All this work on the binary systems was performed before the Fe-B-Cr description by Yamada et al. [2] was published and in accordance with the above mentioned strategy to form a simple and compatible thermodynamic database for steels.

\* AALTO UNIVERSITY, SCHOOL OF CHEMICAL TECHNOLOGY, ESPOO, FINLAND

\*\* UNIVERSITY OF PLOVDIV, FACULTY OF CHEMISTRY, PLOVDIV, BULGARIA

## 2. Phases, modeling and data

Detailed descriptions of the substitutional solution and sublattice models and their parameters are available in the literature [6, 7] and in this journal (Vassilev and Lilova [8]). Therefore, abbreviated descriptions of the phases and models are presented only (TABLE 1). The solution phases (L, bcc\_A2 (bcc), fcc\_A1 (fcc)) are described with the substitutional solution model. The various Fe- and Cr-borides are generally described using sublattice models taking into account the reciprocal solubility of the third constituent (Fe or Cr) and three of them (Cr<sub>3</sub>B<sub>4</sub>, CrB<sub>2</sub> and CrB<sub>4</sub>) are treated as stoichiometric phases. The sigma ( $\sigma$  or (Fe)<sub>8</sub>(Cr)<sub>4</sub>(Cr,Fe)<sub>18</sub>) phase is described with the sublattice model as well. No solubility of neither Fe nor Cr in the rhombohedral boron phase (referred to as "bet" below) is assumed.

TABLE 1  
Phases and their modeling in the present Fe-B-Cr description

Phase	Modeling
liquid (L)	(B,Cr,Fe), substitutional, RKM <sup>a</sup>
bcc_A2 (bcc)	(B,Cr,Fe), substitutional, RKM <sup>a</sup>
fcc_A1 (fcc)	(B,Cr,Fe), substitutional, RKM <sup>a</sup>
Sigma ( $\sigma$ )	(Fe) <sub>8</sub> (Cr) <sub>4</sub> (Cr,Fe) <sub>18</sub> , sublattice, RKM <sup>a</sup>
Fe <sub>2</sub> B (dissolving Cr)	(Cr,Fe) <sub>2</sub> (B), sublattice, RKM <sup>a</sup>
FeB (dissolving Cr)	(Cr,Fe)(B), sublattice, RKM <sup>a</sup>
Cr <sub>2</sub> B (dissolving Fe)	(Cr,Fe) <sub>2</sub> (B), sublattice, RKM <sup>a</sup>
Cr <sub>3</sub> B <sub>3</sub> (dissolving Fe)	(Cr,Fe) <sub>5</sub> (B) <sub>3</sub> , sublattice, RKM <sup>a</sup>
CrB (dissolving Fe)	(Cr,Fe)(B), sublattice, RKM <sup>a</sup>
Cr <sub>3</sub> B <sub>4</sub>	(Cr) <sub>3</sub> (B) <sub>4</sub> , stoichiometric
CrB <sub>2</sub>	(Cr)(B) <sub>2</sub> , stoichiometric
CrB <sub>4</sub>	(Cr)(B) <sub>4</sub> , stoichiometric
beta-rhombo-B (bet)	(B)

<sup>a</sup> – RKM = Redlich-Kister-Muggianu expression  
(excess Gibbs energy model)

The experimental studies on the Fe-B-Cr system until 1992 have been reviewed by Raghavan [9]. TABLE 2 shows the experimental data for the Fe-B-Cr system selected in the current optimization. Additionally, the experimental data of Fe-B phase equilibria [10-15], the mixing enthalpy of liquid Fe-B alloys [16, 17], the activity of Fe and B in liquid Fe-B alloys [18, 19], the enthalpy of formation of Fe<sub>2</sub>B and FeB [20, 21], B-Cr phase equilibria [22, 23], the mixing enthalpy in liquid B-Cr alloys [17], and the enthalpy of formation of chromium borides [23-25] were used in the partial re-optimization of the Fe-B and B-Cr systems.

TABLE 2  
Experimental data applied in the optimization for the Fe-B-Cr system

Experimental data	Reference
Liquidus projection	[9, 26]
5 isothermal sections, at 1100, 1000, 900, 800 and 700°C	[26-29]
Enthalpy of mixing of liquid alloys, at 1877°C	[17]
Activity coefficient $\gamma_B^{Cr}$ in liquid alloys, at 1600°C	[30]

## 3. Results

The thermodynamic description of the Fe-B-Cr system is presented in TABLE 3. The parameters marked with a reference code were taken from earlier assessments and those marked with O\* or E\*, respectively, were optimized using literature experimental data (TABLE 2) or estimated when no experimental data are available.

TABLE 3  
Thermodynamic description of the Fe-B-Cr system. Thermodynamic data of the pure components are given by [31, 32] unless not shown in the table. Parameter values except for Tc and  $\beta$  are in J/mol

<b>liquid</b> (1 sublattice, sites: 1, constituents: B,Cr,Fe)	<b>Ref.</b>
$L_{B,Cr}^L = (-134482+26.8T) + (+14347)(x_B-x_{Cr}) + (-1674)(x_B-x_{Cr})^2 + (-43361)(x_B-x_{Cr})^3$	[5]
$L_{B,Fe}^L = (-133438+33.946T) + (+7771)(x_B-x_{Fe}) + (+29739)(x_B-x_{Fe})^2$	[3]
$L_{Cr,Fe}^L = (-17737+7.997T) + (-1331)(x_{Cr}-x_{Fe})$	[4]
$L_{B,Cr,Fe}^L = (-90000-20T)x_B + (-60000-20T)x_{Cr} + (120000-20T)x_{Fe}$	O*
<b>bcc</b> (1 sublattice, sites: 1, constituents: B,Cr,Fe)	
${}^oG_B^{bcc} = {}^oG_B^{bet} + (+43514-12.217T)$	[32]
$L_{B,Cr}^{bcc} = (-37000)$	O*
$L_{B,Fe}^{bcc} = (-50000+42T)$	O*
$L_{Cr,Fe}^{bcc} = (+20500-9.68T)$	[33]
$Tc^{bcc} = 1043x_{Fe}-311x_{Cr}+x_{Fe}x_{Cr}(1650-550(x_{Fe}-x_{Cr}))$	[33]
$\beta^{bcc} = 2.22x_{Fe}-0.008x_{Cr}-0.85x_{Fe}x_{Cr}$	[33]

<b>fcc</b> (1 sublattice, sites: 1, constituents: B,Cr,Fe) ${}^oG_B^{fcc} = {}^oG_B^{bet} + (+50208-13.478T)$ $L_{B,Cr}^{fcc} = L_{B,Cr}^{bcc}$ (fcc not stable in binary B-Cr) $L_{B,Fe}^{fcc} = (-66000+50T)$ $L_{Cr,Fe}^{fcc} = (+10833-7.477T) + (+1410)(x_{Cr}-x_{Fe})$ $L_{B,Cr,Fe}^{fcc} = (0)x_B + (0)x_{Cr} + (-220000+50T)x_{Fe}$ $Tc^{fcc} = -201x_{Fe}-1109x_{Cr}$ $\beta^{fcc} = -2.1x_{Fe}-2.46x_{Cr}$	 [32] E* O* [33] O* [31] [31]
<b>Sigma</b> ( $\sigma$ ) (3 sublattices, sites: 8:4:18, constituents: Fe:Cr:Cr,Fe) ${}^oG_{Fe:Cr:Cr}^{\sigma} = 8{}^oG_{Fe}^{fcc} + 22{}^oG_{Cr}^{bcc} + (+92300-95.96T)$ ${}^oG_{Fe:Cr:Fe}^{\sigma} = 8{}^oG_{Fe}^{fcc} + 4{}^oG_{Cr}^{bcc} + 18{}^oG_{Fe}^{bet} + (+117300-95.96T)$	 [33] [33]
<b>Fe<sub>2</sub>B</b> (2 sublattices, sites: 0.6667:0.3333, constituents: Cr,Fe:B) ${}^oG_{Cr:B}^{Fe2B} = 0.6667{}^oG_{Cr}^{bcc} + 0.3333{}^oG_B^{bet} + (-6000+5T)$ ${}^oG_{Fe:B}^{Fe2B} = 0.6667{}^oG_{Fe}^{bcc} + 0.3333{}^oG_B^{bet} + (-26261+3.466T)$ $L_{Cr,Fe:B}^{Fe2B} = (-42000)$	 O* [3] O*
<b>FeB</b> (2 sublattices, sites: 0.5:0.5, constituents: Cr,Fe:B) ${}^oG_{Cr:B}^{FeB} = 0.5{}^oG_{Cr}^{bcc} + 0.5{}^oG_B^{bet} + (-10000+5T)$ ${}^oG_{Fe:B}^{FeB} = 0.5{}^oG_{Fe}^{bcc} + 0.5{}^oG_B^{bet} + (-35150+6T)$ $L_{Cr,Fe:B}^{FeB} = (-45000)$	 O* O* O*
<b>Cr<sub>2</sub>B</b> (2 sublattices, sites: 0.6667:0.3333, constituents: Cr,Fe:B) ${}^oG_{Cr:B}^{Cr2B} = 0.5{}^oG_{Cr}^{bcc} + 0.5{}^oG_B^{bet} + (-30848+1.48T)$ ${}^oG_{Fe:B}^{Cr2B} = 0.5{}^oG_{Fe}^{bcc} + 0.5{}^oG_B^{bet} + (-6000+5T)$ $L_{Cr,Fe:B}^{Cr2B} = (-85000+20T)$	 [5] O* O*
<b>Cr<sub>5</sub>B<sub>3</sub></b> (2 sublattices, sites: 0.625:0.375, constituents: Cr,Fe:B) ${}^oG_{Cr:B}^{Cr5B3} = 0.625{}^oG_{Cr}^{bcc} + 0.375{}^oG_B^{bet} + (-34251+2.257T)$ ${}^oG_{Fe:B}^{Cr5B3} = 0.625{}^oG_{Fe}^{bcc} + 0.375{}^oG_B^{bet}$ $L_{Cr,Fe:B}^{Cr5B3} = (-92500+32T)$	 [5] O* O*
<b>CrB</b> (2 sublattices, sites: 0.5:0.5, constituents: Cr,Fe:B) ${}^oG_{Cr:B}^{CrB} = 0.5{}^oG_{Cr}^{bcc} + 0.5{}^oG_B^{bet} + (-40000+3.24T)$ ${}^oG_{Fe:B}^{CrB} = 0.5{}^oG_{Fe}^{bcc} + 0.5{}^oG_B^{bet} + (-10000+5T)$ $L_{Cr,Fe:B}^{CrB} = (-60000+20T) + (-40000+20T)(y_{Cr}-y_{Fe})$	 O* O* O*
<b>Cr<sub>3</sub>B<sub>4</sub></b> (2 sublattices, sites: 0.4286:0.5714, constituents: Cr:B) ${}^oG_{Cr:B}^{Cr3B4} = 0.4286{}^oG_{Cr}^{bcc} + 0.5714{}^oG_B^{bet} + (-42984+4.95T)$	 [5]
<b>CrB<sub>2</sub></b> (2 sublattices, sites: 0.3333:0.6667, constituents: Cr:B) ${}^oG_{Cr:B}^{CrB2} = 0.3333{}^oG_{Cr}^{bcc} + 0.6667{}^oG_B^{bet} + (-39687+4.184T)$	 [5]
<b>CrB<sub>4</sub></b> (2 sublattices, sites: 0.2:0.8, constituents: Cr:B) ${}^oG_{Cr:B}^{CrB4} = 0.2{}^oG_{Cr}^{bcc} + 0.8{}^oG_B^{bet} + (-24950+3.15T)$	 O*

O\* – Parameter optimized in this work

E\* – Parameter estimated in this work

The calculated results are compared with the original experimental data to verify the optimization. All calculations were carried out using ThermoCalc software [34].

The Fe-Cr phase diagram calculated by [4] and those of Fe-B and B-Cr systems calculated in the current study are shown on Figs. 1-3. The agreement between the optimization results and the experimental data is reasonable, as shown in

the original paper of [4] for Fe-Cr and in Figures 2 and 3 for Fe-B and B-Cr.

The maximum boron content of bcc- and fcc- Fe-B solid solutions (Fig. 1) is slightly higher than the one calculated by Halleman et al. [3]. This result agrees well with the most recent measurements [12, 14]. According to the earlier investigations [35-37], the maximum boron content in the above

mentioned phases is even higher, but those measurements can be considered not accurate enough. The present Fe-B description also gives a slightly lower melting temperature of FeB phase than the one assessed by Hallems et al. [3]. The newly calculated value (1624°C) is lower than that of [3] by 9°C but agrees well with the experimental values of 1590°C by Sidorenko et al. [13] and 1650°C by Portnoi et al. [10]. One has to be aware that all experimental values possess certain inaccuracy due to the errors of the measurements.

Regarding the B-Cr system, only small differences were found between the phase equilibria calculated in this study and those obtained by Campbell and Kattner [5]. A slightly better agreement is observed (Fig. 2) for the  $CrB_2 + bet + CrB_4$  equilibrium whereas the re-optimization of the CrB phase has a visible effect on the Fe-B-Cr system only.

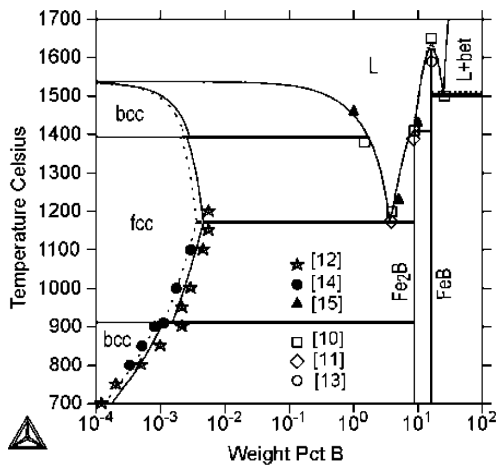


Fig. 1. Fe-B phase diagram calculated with the parameters obtained in this work, together with experimental [12, 14, 15] and assessed [10, 11, 13] data points. Solid lines refer to the present calculations and dotted lines refer to those of [3]

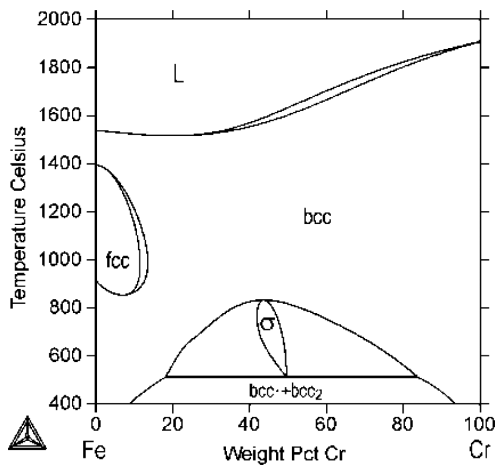


Fig. 2. Fe-Cr phase diagram calculated with the parameters of Lee [4]

In both binaries, Fe-B and B-Cr, good or reasonable agreement was obtained also between the calculated and the experimental mixing enthalpies and component activities in the liquid phase, as well as the borides enthalpies of formation (the references for the respective experimental data are given in Section 2). In each case, the results are identical or

almost identical with those of Hallems et al. [3] for Fe-B and of Campbell and Kattner [5] for B-Cr.

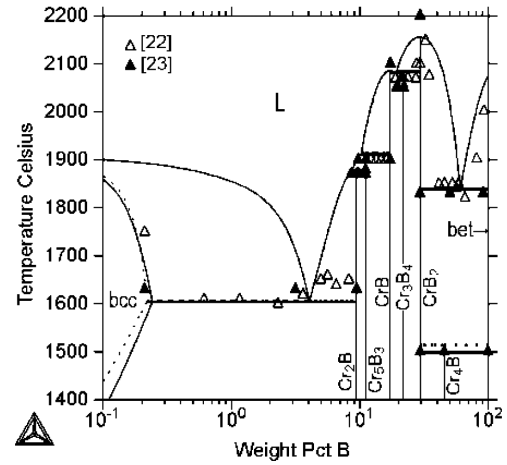


Fig. 3. B-Cr phase diagram calculated with the parameters obtained in this work, together with experimental data points [22, 23]. Solid lines refer to the present calculations and dotted lines refer to those of [5]

Figures 4-12 and TABLE 4 show a reasonably good agreement between the calculated results and the experimental data for the Fe-B-Cr system (TABLE 2). In the liquidus projection (Fig. 4) and TABLE 4, small inconsistency in the location of point  $U_5$  exists indicating that the calculated fcc-surface is narrower than experimentally observed one. Moreover, it should be noted that the composition values for points  $U_1$ ,  $U_2$  and  $U_3$  are estimated by [9] and are not experimentally obtained.

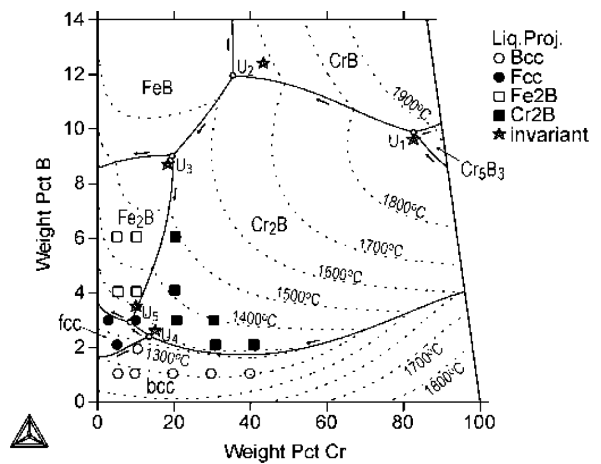


Fig. 4. Calculated liquidus projection of the Fe-B-Cr system, together with the experimental data points [26, 9]. The calculated liquidus isotherms between 1300 and 1900°C (dotted lines) are shown too

Five isothermal sections of the system, shown in Figures 5-9 agree reasonably well with the experimental data. In Figure 5, however, a disagreement of the mutual solubilities (see the experimental one-phase symbols in the calculated two-phase lines of the  $FeB + CrB$  and  $Fe_2B + Cr_2B$  equilibria) is observed.

TABLE 4

Calculated (calc) and experimental (exp) invariant points in the Fe-B-Cr system. Code – reaction type, U – unknown; t – temperature, °C

Reaction	Code	t °C	wt % Cr in L	wt % B in L	Reference
L+Cr <sub>5</sub> B <sub>3</sub> =Cr <sub>2</sub> B+CrB	U <sub>1</sub>	1860	82.69	9.89	calc This study
		–	82.6*	9.6*	exp [9]
L+CrB=Cr <sub>2</sub> B+FeB	U <sub>2</sub>	1613	35.43	11.95	calc This study
		–	43.5*	12.4*	exp [9]
L+FeB+Cr <sub>2</sub> B=Fe <sub>2</sub> B	U <sub>3</sub>	1521	19.70	9.04	calc This study
L+FeB=Cr <sub>2</sub> B+Fe <sub>2</sub> B		–	18.3*	8.7*	exp [9]
L+bcc=Cr <sub>2</sub> B+fcc	U <sub>4</sub>	1263	13.47	2.44	calc This study
		1270	15.0	2.6	exp [9]
L+Cr <sub>2</sub> B=Fe <sub>2</sub> B+fcc	U <sub>5</sub>	1229	8.67	2.92 3.5	calc This study
		1226	10.0		exp [9]

\* – Estimated value

The calculated enthalpy of mixing and activity coefficient of  $\gamma_B^{Cr}$  in liquid alloys are shown in Figures 10 and 11, respectively. The agreement with the experimental data is reasonable. Finally, Figure 12 presents the calculated B solubility in the ternary fcc and bcc phases. It can be concluded that Cr content increase promotes the formation of Cr<sub>2</sub>B, thus decreasing the B content of the solid solutions. That content is reduced also by the temperature drop from 1150 to 1000°C.

Additional experimental data for the phase equilibria of the system are available from [38] and [39] but these results are relatively inconsistent with the other experimental data and the calculations. The isotherm of 1250°C [38] shows no liquid phase, which should be presented at this temperature, and the FeB-CrB section by [39] shows too high solubilities of the third constituents (i.e. Cr in FeB and Fe in CrB), in comparison with the measurements [27, 28].

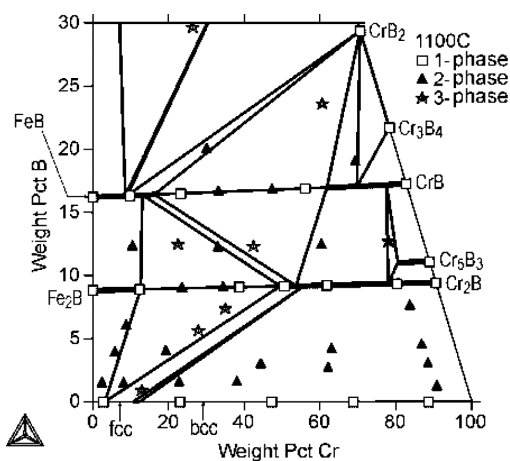


Fig. 5. Calculated isotherm of 1100°C in the Fe-B-Cr system, together with experimental data points [28]

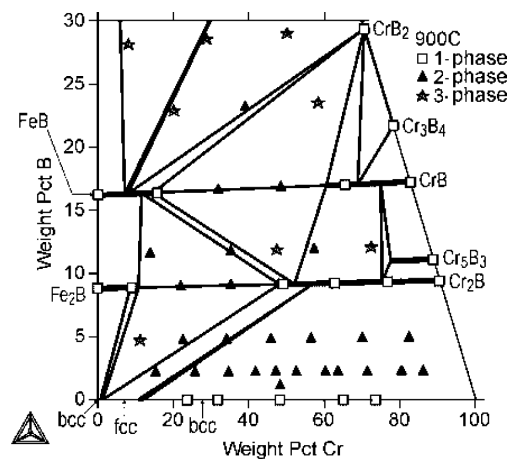


Fig. 7. Calculated isotherm at 900°C in the Fe-B-Cr system, together with experimental data points [27]

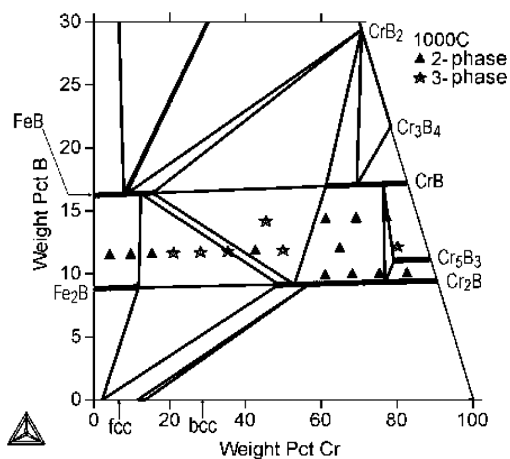


Fig. 6. Calculated isotherm at 1000°C in the Fe-B-Cr system, together with experimental data points [29]

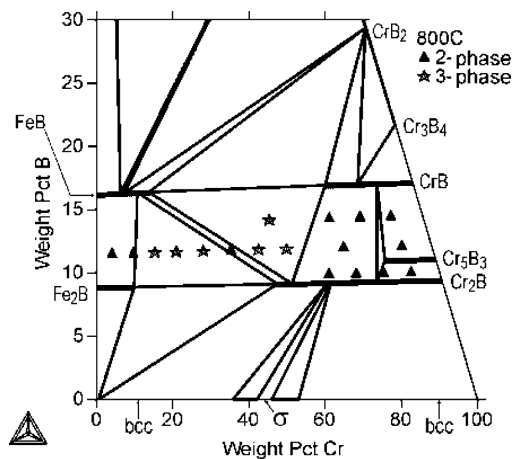


Fig. 8. Calculated isotherm at 800°C in the Fe-B-Cr system, together with experimental data points [29]

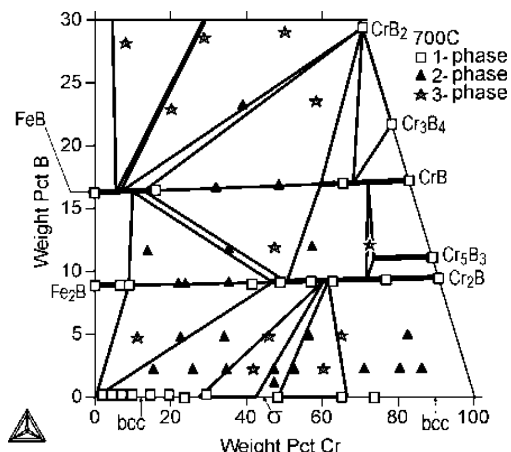


Fig. 9. Calculated isotherm at 700°C in the Fe-B-Cr system, together with experimental data points [26, 27]

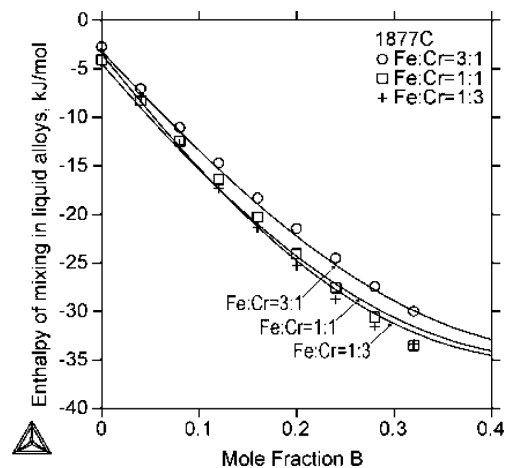


Fig. 10. Calculated molar enthalpy of mixing of liquid Fe-B-Cr alloys at 1877°C, together with experimental data points [17]. The reference states used are pure liquid components

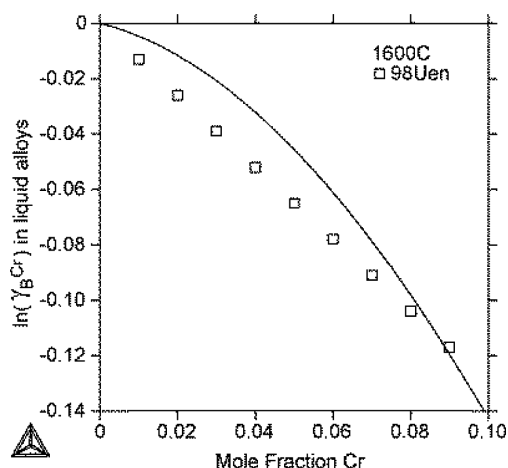


Fig. 11. Calculated activity coefficient  $\gamma_B^{Cr}$  in liquid Fe-B-Cr alloys at 1600°C, together with smoothed experimental data points [30]

It is worth of noting that the current Fe-B-Cr description gives quite different results than those of Yamada et al. [2]. For example (Fig. 4), the primary  $\text{Fe}_2\text{B}$  surface calculated by the latter authors [2] extends to rather high Fe contents in the Fe-rich corner of the system, with regard to the present

calculations and the experimental and assessed data points of [26, 9]. The most essential difference, however, is the much wider FeB and  $\text{Cr}_5\text{B}_3$  surfaces [2], compared with the current results and the assessed liquidus projection [9].

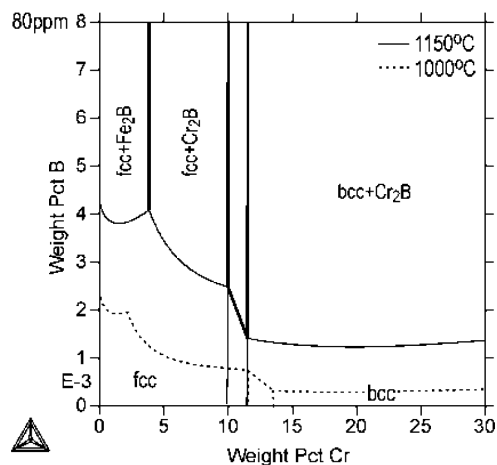


Fig. 12. Calculated B solubility in the fcc and bcc phases of the Fe-B-Cr system, at 1150 and 1000°C

Additionally, there are differences in the calculated isothermal sections (see Figures 5 to 9), although a reasonable agreement is obtained between both descriptions. In addition, the results of Yamada et al. [2] with regards to the molar enthalpy of mixing of liquid Fe-B-Cr alloys (Fig. 10) and the calculated chromium activity coefficient in liquid alloys (Fig. 11), deviate from the present ones and the experimental data [17, 30]. The mixing enthalpies [2] are slightly stronger in negative direction than those shown in Fig. 10 whereas those of the activity coefficient  $\gamma_B^{Cr}$  [2] have positive values being beyond the figure scale. On the other hand, the description of Yamada et al. [2] gives a reasonable prediction for the experimental FeB-CrB section [39] whereas the present description does not. However, due to the special scope of the present Fe-B-X database to provide reliable results at low B contents, no attempts were made to improve that agreement.

#### 4. Summary

A thermodynamic optimization of the ternary Fe-B-Cr system was performed using experimental thermodynamic and phase equilibrium data from the literature. In this description, twelve phases, i.e., liquid, bcc, fcc, sigma,  $\text{Fe}_2\text{B}$  (dissolving Cr), FeB (dissolving Cr),  $\text{Cr}_2\text{B}$  (dissolving Fe),  $\text{Cr}_5\text{B}_3$  (dissolving Fe), CrB (dissolving Fe),  $\text{Cr}_3\text{B}_4$ ,  $\text{CrB}_2$ ,  $\text{CrB}_4$  and beta-rhombo-B, were considered. Partial reoptimizations of the binary Fe-B and Cr-B systems have been done in order to make the descriptions compatible with the new thermodynamic database of Fe-B-X systems. Good or reasonable agreement was obtained between the calculated and the experimental thermodynamic and phase equilibrium data. The differences of the present optimizations with an earlier one have been discussed.

### Acknowledgements

Financial support of the Technology Development Centre (TEKES) during the Elemet Mocaastro III project is gratefully acknowledged by Dr J. Miettinen.

### REFERENCES

- [1] W. Wang, S. Zhang, X. He, *Acta Metall. Mater.* **43**, 1693 (1995).
- [2] K. Yamada, H. Ohtani, M. Hasebe, *High Temp. Mat. and Proc.* **27**, 269 (2008).
- [3] B. Hallemaans, J.R. Wollants, Z. Roos, *Metallkd.* **85**, 676 (1994).
- [4] B.-J. Lee, *CALPHAD* **17**, 251 (1993).
- [5] C.E. Campbell, U.R. Kattner, *CALPHAD* **26**, 477 (2002).
- [6] C. Qiu, *ISIJ International* **32**, 1117 (1992).
- [7] C. Qiu, Thermodynamic study of carbon and nitrogen in stainless steels. PhD thesis, Royal Institute of Technology, Stockholm, 1993.
- [8] G. Vassilev, K. Lilova, *Arch. Metall. Mater.* **51**, 365 (2006).
- [9] V. Raghavan, Phase Diagrams of Ternary Iron Alloys – Part 6A, Indian Institute of Metals, Calcutta, 1992.
- [10] K.I. Portnoi, M.Kh. Levinshkaya, V.M. Romashov, *Sov. Powder Metall. Met. Ceram.* **8**, 657 (1969).
- [11] L.G. Voroshin, L.S. Lyakhovich, G.G. Panich, G.F. Protasevich, *Met. Sci. Heat Treat. (USSR)* **9**, 732 (1970).
- [12] A. Brown, J.D. Garnish, R.W.K. Honeycombe, *Metall. Sci.* **8**, 317 (1974).
- [13] F.A. Sidorenko, N.N. Serebrennikov, V.D. Budozhanov, Yu.V. Putintsev, S.N. Trushevskii, V.D. Korabanova, V. Geld, *High Temp.* **15**, 36 (1977).
- [14] T.B. Cameron, J.E. Morral, *Metall. Trans. A* **17A**, 1481 (1986).
- [15] N.A. Vatolin, A.L. Zavialov, V.I. Zhuchkov, *J. Less Common Met.* **117**, 91 (1986).
- [16] P.V. Geld, Yu.O. Esin, V.M. Baev, *Conf. Int. Thermodyn. Chim.* **3**, 248 (1975).
- [17] V.T. Witusiewicz, *Thermochimica Acta* **264**, 41 (1995).
- [18] M. Yukinobu, O. Ogawa, S. Goto, *Metall. Trans. B* **20B**, 705 (1989).
- [19] T. Miki, K. Tsujita, S. Ban-Ya, M. Hino, *Calphad* **30**, 449 (2006).
- [20] O.S. Gorelkin, A.S. Dubrovin, O.D. Kolesnikova, N.A. Chirkov, *Russ. J. Phys. Chem.* **46**, 431 (1972).
- [21] S. Sato, O.J. Kleppa, *Metall. Trans. B* **13B**, 251 (1982).
- [22] K.I. Portnoi, V.M. Romashov, *Poroshk. Metall.* **113**, 48 (1972).
- [23] P.K. Liao, K.E. Spear, *Bull. Alloy Phase Diagrams* **7**, 232 (1986).
- [24] K. Hack, T.G. Chart, Estimation and Critical Assessment of Thermodynamic Data for the B-Cr System, Div. Mater. Appl. Natl. Phys. Lab. Teddington, UK, Comm. Eur. Communities, EUR 7820, Pt. 2, 1982.
- [25] L. Topor, O.J. Kleppa, *J. Chem. Thermodyn.* **17**, 109 (1985).
- [26] H. Kaneko, T. Nishizawa, A. Chiba, *Nippon Kinzoku Gakkai-Si.* **30**, 157 (1966).
- [27] M.V. Chepiga, Yu.B. Kuzma, *Izv. VUZ Chern. Metall.* **3**, 127 (1970).
- [28] A.E. Gorbunov, F.M. Bodyryan, *Sborn. Trudov. Vses. Nauchn. Issled. I Proekt. Inst. Tugoplavk. Met. i Tverd. Splavov.* **16**, 172 (1976).
- [29] C. Gianoglio, G. Pradelli, *Atti Accad. Sci. Torino, Cl. Sci. Fis. Met. Nat.* **117**, 391 (1985).
- [30] S. Ueno, Y. Waseda, K.T. Jacob, S. Tamaki, *Steel Research*, 59 (1998) 474-83, by citing “Selected values of thermodynamic properties for steelmaking, The 19<sup>th</sup> Committee, Japan Society for Promotion and Science, 1984”.
- [31] A.T. Dinsdale, SGTE unary database, version 4.4; [www.sgte.org](http://www.sgte.org).
- [32] I. Ansara, A.T. Dinsdale, M.H. Rand, COST 507 – Thermochemical database for light metal alloys, Volume 2, European Communities, Belgium, 1998.
- [33] J.-O. Andersson, B. Sundman, *CALPHAD* **11**, 83 (1987).
- [34] J.-O. Andersson, T. Helander, L. Höglund, P. Shi, B. Sundman, *CALPHAD* **26**, 273 (2002).
- [35] P.E. Busby, M.E. Wurga, C. Wells, *Trans AIME* **197**, 1463 (1953).
- [36] M.E. Nicholson, *Trans AIME* **200**, 185 (1954).
- [37] C.C. McBride, J.W. Spretnak, R. Speiser, *Trans. Amer. Soc. Met.* **46**, 499 (1954).
- [38] M.L. Borlera, G. Pradelli, *Metall. Ital.* **65**, 421 (1973).
- [39] K. Shirae, Y. Ueda, S. Kachi, K. Kosuge, *Mater. Res. Bull.* **22**, 521 (1987).